Photopolymerized Epoxide Copolymer Thin Films with Surfaces Highly Enriched with Sulfonyl Fluoride Groups

A. U. Schnurer, N. R. Holcomb, and G. L. Gard*

Department of Chemistry, Portland State University, Portland, Oregon 97207

D. G. Castner

Department of Chemical Engineering and National Surface Analysis Center for Biomedical Problems, Box 351750, University of Washington, Seattle, Washington 98195-1750

D. W. Grainger*

Department of Chemistry, Colorado State University, Fort Collins, Colorado 80523-1872

Received January 24, 1996. Revised Manuscript Received April 16, 1996[⊗]

Photoinitiated polymerization of fluorinated aliphatic epoxides bearing terminal sulfonyl fluoride groups with a commercial cycloaliphatic diepoxide (Cyracure UVR-6110) results in highly cross-linked glassy films. Depth-dependent surface analysis using XPS shows that these films are highly enriched in their outer molecular surface regions with sulfonyl fluoride groups. Films prepared with 17 wt % and higher sulfonyl fluoride epoxide monomers exhibit compositions close to that of a pure 100% photopolymerized sulfonyl fluoride epoxide monomer in the outer 50 Å of the film. Even a film prepared with 1 wt % sulfonyl fluoride monomer exhibits a few angstroms thick overlayer of sulfonyl fluoride. FTIR (attenuated total reflectance) spectra exhibit infrared signatures consistent with these data. Secondary ion mass spectra exhibit peaks associated with perfluoro and sulfonyl fluoride moieties, supporting overlayer enrichment of these species within the sampling depth of this method (outer 15 Å). Such extreme surface enrichment by the fluorinated epoxide has utility for applications where costly or exotic fluorinated monomers are required to impart a robust overlayer yet comprise only minority component additives of the total polymerization mixture.

Introduction

Polymer surface enrichment is a nonstoichiometric or disproportionate amount of a polymer component, segment, block, or grafted chain at the surface of a polymer film relative to its bulk composition. Surface enrichment in polymers is interesting because, unlike many solid-state materials, a polymer surface may exhibit a drastically different surface composition from its bulk. Such nonstoichiometric surface phenomena are often a function of a noncrystalline polymer's general metastable or mobile nature; polymer chains exhibit relaxation processes resulting in bulk/surface remodeling. In this sense, surface enrichment is thermodynamically driven and kinetically controlled, governed by a polymer's bulk structure, miscibility of its various components, and surface free energy differences between polymer segments or blocks.[1] Polymer surface rearrangement resulting from segmental response to changing external environments (e.g., aqueous to air) have now been documented in numerous studies.[2−16]

We are interested in surface rearrangements of polymer species that result in surface enrichment of a particular chemistry. In a set of original studies,[17−19] Thomas and O'Malley used XPS to confirm surface enrichment in polystyrene/polyethyleneoxide block copolymers. Another classic set of studies was performed by Ratner and co-workers on surface enrichment in polyurethanes.[1,20,21] Other examples of explicit polymer surface enrichment include polystyrene/hydroxyethyl methacrylate block copolymers[22] and poly(dimethylsiloxane)−poly(ethylene oxide)−heparin block copolymers.[23] In all cases, polymer surfaces exposed to air

* To whom correspondence should be addressed.

[⊗] Abstract published in *Advance ACS Abstracts,* June 1, 1996.

(1) Yoon, S. C.; Ratner, B. D. *Macromolecules* **1986**, *19*, 1068.
(2) Lavielle, L.; Schultz, J. *J. Colloid Interface Sci.* **1985**, *106*, 438.
(3) Lavielle, L.; Schultz, J. *J. Colloid Interface Sci.* **1985**, *106*, 446.
(4) Rasmussen, J. R.; Bergbreiter, D. E.; Whitesides, G. M. *J. Am. Chem. Soc.* **1977**, *99*, 4746.
(5) Ruckenstein, E.; Gourisankar, S. V. *J. Colloid Interface Sci.* **1985**, *107*, 488.
(6) Yasuda, H.; Charlson, E. J.; Charlson, E. M.; Yasuda, T.; Miyama, M.; Okuno, T. *Langmuir* **1991**, *7*, 2394.
(7) Ratner, B. D.; Weathersby, P. K.; Hoffman, A. S.; Kelly, M. A.; Scharpen, L. H. *J. Appl. Poly. Sci.* **1978**, *22*, 643.
(8) Takamori, K.; Jo, N.-J.; Takahara, A.; Kajiyama, T. *Rep. Prog. Polym. Phys. Jpn.* **1987**, *30*, 57.
(9) Takahara, A.; Jo, N.-J.; Takamori, K.; Kajiyama, T. In *Progress in Biomedical Polymers*; Plenum: New York, 1990; p 217.
(10) Tingey, K. G.; Andrade, J. D.; Zdrahala, R. J.; Chittur, K. K.; Gendreau, R. M. In *Surface Characterization of Biomaterials*; Ratner, B. D., Ed.; Elsevier: Amsterdam, 1988; p 255.
(11) Deng, Z.; Schreiber, H. P. *J. Adhesion* **1991**, *36*, 71.
(12) Teraya, T.; Takahara, A.; Kajiyama, T. *Polymer* **1990**, *31*, 1149.
(13) Holly, F. J.; Refojo, M. F. *ACS Symp. Series* **1976**, *31*, 252.
(14) Holly, F. J.; Refojo, M. F. *J. Biomed. Mater. Res.* **1975**, *9*, 315.
(15) Andrade, J. D.; King, R. N.; Gregonis, D. E. *ACS Symp. Ser.* **1976**, *31*, 206.
(16) Lee, S. H.; Ruckenstein, E. *J. Colloid Interface Sci.* **1987**, *120*, 529.
(17) Clark, D. T.; Dilks, A.; Peeling, J.; Thomas, H. R. *J. Chem. Soc. Faraday Discuss.* **1975**, *60*, 183.
(18) Thomas, H. R.; O'Malley, J. J. *Macromolecules* **1979**, *12*, 323.
(19) O'Malley, J. J.; Thomas, H. R.; Lee, G. M. *Macromolecules* **1979**, *12*, 996.
(20) Yoon, S. C.; Ratner, B. D. *Macromolecules* **1988**, *21*, 2392.
(21) Yoon, S. C.; Ratner, B. D. *Macromolecules* **1988**, *21*, 2401.
(22) Castner, D. G.; Ratner, B. D.; Grainger, D. W.; Kim, S. W.; Okano, T.; Suzuki, K.; Briggs, D.; Nakahama, S. *J. Biomater. Sci., Polym. Ed.* **1992**, *3* 463.

S0897-4756(96)00049-X CCC: $12.00

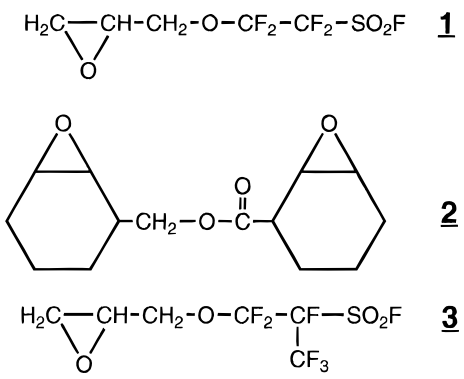

Figure 1. Structures of the three epoxide monomers used for film photopolymerization.

were enriched in polymer segments of the lowest interfacial free energy, indicating polymer surface rearrangement to accommodate thermodynamic driving forces.

Because of their intrinsically low surface free energy, perfluorinated chains are known to enrich polymer interfaces.[24−26] From a practical standpoint, such a phenomenon is both fundamentally interesting and technologically attractive: inexpensive bulk aliphatic polymer resins "doped" with small amounts of high value-added fluorinated monomers could yield polymeric fluorinated surface overlayers of substantially different chemical and physical properties from the bulk polymer matrix. We have recently been able to extend this perfluorocarbon-enrichment architectural principle to polymer monolayer films on surfaces.[24] We now report this fluorinated surface enrichment phenomenon in bulk epoxyfluorocarbon sulfonyl fluorides. Synthesis and preliminary polymerization results of the aliphatic epoxide fluorocarbon sulfonyl fluoride, shown in Figure 1, were reported earlier.[27,28] These initial studies provided early evidence for fluorinated monomer enrichment, based on contact angle (wetting) results.

We have used angle-dependent X-ray photoelectron spectroscopy (XPS) and secondary ion mass spectrometry (SIMS) in the current study to provide unambiguous quantitation of fluoroepoxide enrichment in the surface regions of these films copolymerized with a commercial cycloaliphatic diepoxide. Because of the interest in fluorocarbon sulfonyl fluorides as new surfactants, ion-exchange resins, precursors for sulfonic acids,[29−32] as well as low-refractive index materials, photopolymerization of these monomers into polymer films and their resulting interfacial properties should lead to interesting applications of these new robust fluorinated coatings.

Experimental Section

Materials. The sulfonyl fluoride-containing epoxide OCH_2-$CHCH_2OCF_2CF_2SO_2F$ (**1**, see Figure 1) was prepared according to the literature method.[27] A related fluorinated sulfonyl fluoride monomer (**3**) was also synthesized.[33] The cross-linking agent Cyracure UVR-6110, a cycloaliphatic diepoxide (**2**), and the photoinitiator UVI-6990, a triarylsulfonium hexafluorophosphonate salt (50 wt % clear, amber solution in propylene carbonate), were donated by the Union Carbide Chemicals and Plastics Co. and used as received.

General Polymerization Procedures. Fluorinated epoxides **1** or **3** and Cyracure UVR-6110 (**2**) were mixed in various proportions (designated by weight percent composition with regard to total monomer content). Photoinitiator UVI-6990 solution was added (constant 2.0 wt %) to all monomer mixtures. Photoinitiated polymerizations were performed using clean glass or brass substrates on which films of nominally 15 μm wet thickness were cast and drawn down as thin films using a no. 10 Meyer rod. In all cases, the films were annealed at elevated temperatures (55 °C) prior to photocuring. The coated substrates were irradiated in a horizontal position using a 450 W Hanovia mercury lamp passed through a quartz water-filled heat filter to an aluminum parabolic reflector for various times under nitrogen at 25 cm distance. These conditions provided a controlled polymerization environment limiting possible variations due to changing humidity, ozonolysis, and atmospheric contamination.

Characterization of Photopolymerized Epoxide Films. *Fourier Transform Infrared Spectroscopy (FTIR).* Attenuated total reflectance FTIR spectra were collected on a Nicolet 60SX instrument with a liquid N_2 cooled MCT detector using a Spectratech variable-angle ATR accessory at normal incident angle onto a KRS-5 crystal (50 mm × 10 mm, face angles = 45°). Bare substrates were used as references. Films on substrates or bare substrates were pressed against the ATR prism to maximize interfacial contact. Spectra were taken at 4 cm^{-1} resolution with 1024 scans. Reference subtraction and flattening were achieved using Spectracalc software (Galactic Ind.), but no curve smoothing or other alterations were used.

X-ray Photoelectron Spectroscopy. X-ray photoelectron spectroscopy (XPS) experiments were performed on a Surface Science SSX-100 spectrometer (Mountain View, CA) equipped with a monochromatic Al Kα source, hemispherical analyzer, and a multichannel detector. Typically, spectra were collected with the analyzer at 55° with reference to the sample surface normal, and the operating pressure was approximately 3 × 10^{-9} Torr. High-resolution spectra were obtained at a pass energy of 50 eV using a 1000 μm spot size. Both survey spectra and data for quantitative analysis were collected at a pass energy of 150 eV and a spot size of 1000 μm. The binding energy (BE) scales for all spectra were referenced to the C_{1s} C−H peak at 285.00 eV. Peak fitting of the high-resolution spectra was done using Gaussian peak shapes with commercial software supplied by Surface Science Instruments. For calculation of XPS elemental composition, the analyzer transmission function was assumed not to vary with photoelectron kinetic energy (KE),[34] the photoelectron escape depth was assumed to vary as $KE^{0.7}$,[34] and Scofield's photoionization cross sections were used.[35]

Angle-dependent XPS data were collected at nominal photoelectron takeoff angles of 0°, 55°, and 80°. The takeoff angle was defined as the angle between the surface normal and the axis of the analyzer lens system. Using mean free paths calculated from the equations given by Seah and Dench,[36] the sampling depth (3 times the mean free path) for C_{1s} photoelectrons should decrease from 90 to 15 Å as the takeoff angle increases from 0° to 80°. From analysis of replicates, the

(23) Grainger, D. W.; Okano, T.; Kim, S. W.; Castner, D. G.; Ratner, B. D.; Briggs, D.; Sung, Y. K. *J. Biomed. Mater. Res.* **1990**, *24*, 547.
(24) Sun, F.; Castner, D. G.; Mao, G.; Wang, W.; McKeown, P.; Grainger, D. W. *J. Am. Chem. Soc.* **1996**, *118*, 1856.
(25) Dorff, M. M.; Lindner, E. *Macromolecules* **1989**, *22*, 2951.
(26) Hopken, J.; Sheiko, S.; Czech, J.; Möller, M. *Polym. Prepr. (Am. Chem. Soc., Div. Polym. Chem.)* **1992**, 937.
(27) Chen, L. F.; Mohtasham, J.; Gard, G. L. *J. Fluorine Chem.* **1990**, *46*, 39.
(28) Hamel, N. N.; Russell, G. A.; Gard, G. L. *J. Fluorine Chem.* **1994**, *66*, 105.
(29) Olah, G. A.; Iyer, P. S.; Sura, P. *Synthesis* **1986**, 513.
(30) Hamel, N.; Gard, G. L. *J. Fluor. Chem.* **1994**, *68*, 253.
(31) Canich, J. M.; Ludvig, M. M.; Gard, G. L.; Shreeve, J. M. *Inorg. Chem.* **1984**, *23*, 4403.
(32) Terjeson, R. J.; Mohtasham, J.; Sheets, R. M.; Gard, G. L. *J. Fluorine Chem.* **1988**, *38*, 3.
(33) Chen, L. F.; Mohtasham, J.; Gard, G. L. *J. Fluorine Chem.* **1990**, *48*, 107.
(34) Application note from Surface Science Instruments, Mountain View, CA, 1987.
(35) Scofield, J. H. *J. Electron. Spectrosc. Related. Phenom.* **1976,** *8*, 129.
(36) Seah, M. P.; Dench, W. A. *Surf. Interface Anal.* **1979**, *1*, 2.

typical XPS uncertainties were observed to be less than ±1.0 atom % for carbon and fluorine, less than ±0.5 atom % for oxygen and less than ±0.3 atom % for sulfur.

Quadrupole Static Secondary Ion Mass Spectrometry. Static secondary ion mass spectrometry (SIMS) experiments were performed with a Physical Electronics 3700 SIMS system (Eden Prairie, MN) mounted on a custom ultrahigh-vacuum (UHV) system. The ion beam was rastered over a 5 × 5 mm area, and the total exposure time of the sample to the ion beam, including setup and data acquisition, was less than 7 min. Corresponding total ion doses per sample ($<5 \times 10^{12}$ ions/cm^2) are within the generally accepted limit for static SIMS conditions for organic surfaces.[23] Both positive and negative secondary ions were collected over a *m*/*z* range of 0 to 300 with a nominal mass resolution of unity. Data acquisition and control of the energy filter and quadrupole used the Physical Electronics SIMS software package.

The UHV system has a turbomolecular and Ti sublimation pumped analysis chamber with an *XYZ*Θ sample manipulator. The base pressure in this chamber is 1×10^{-10} Torr. Samples are transferred into the analysis chamber from a turbomolecular-pumped sample introduction chamber. The PHI SIMS system contains a 90° adjustable energy filter and Balzers 0-511 amu quadrupole mass spectrometer for detection of positive and negative secondary ions emitted by the sample. A differentially pumped Leybold-Heraeus (Koln, Germany) ion source was used to produce a 0.5 nA, 3.5 keV Xe^+ primary ion beam.

Contact Angle Analysis. Sessile drop contact angle analysis (Ramé-Hart 100 apparatus) used purified (Millipore 18 MΩ cm resistivity) water drops (2 μL) on three separate spots on each film surface in a controlled environment (100% relative humidity). Measurements were taken on both sides of water drops at ambient temperature 30−40 s after drops were applied to surfaces. Contact angle data report the average of three drops at different surface locations.

Results and Discussion

Fluorinated epoxide **1** is known to readily polymerize via various mechanisms, including photocatalyzed cationic initiation.[28] Additionally, previous work has also shown that epoxide **1** will copolymerize with the commercial cycloaliphatic diepoxide **2** via photoinitiated polymerization to yield cross-linked copolymer films from cast, neat monomer mixtures.[28] Polymerization of the analogous fluorinated epoxide **3** is presumed to proceed via similar mechanisms in both homo- and copolymerizations. The ready transformation of viscous liquid monomer mixtures to insoluble robust, hardened polymer films after several minutes of UV irradiation supports this presumption. Polymerized films were generally transparent and continuous at all monomer compositions after polymerization.

Polymerized films on substrates interrogated by ATR-FTIR displayed spectral features consistent with their chemical structure.[37] Figure 2 shows spectra for copolymerized films comprising (A) 50 wt % fluorinated epoxide **3** and 48 wt % aliphatic diepoxide **2**, (B) 1 wt % fluorinated epoxide **3** and 97 wt % diepoxide **2**, (C) 50 wt % fluorinated epoxide **1** and 48 wt % diepoxide **2**, and (D) 1 wt % fluorinated epoxide **1** and 97 wt % diepoxide **2**. Prominent spectral features include the following: hydroxyl −OH stretch (2° ring-opened alcohol) at 3693 and 3619 cm^{-1}; hydrocarbon asymmetric and symmetric stretch (−CH_2−) at 2916 and 2850 cm^{-1}, respectively; carbonyl stretch of the ester in aliphatic diepoxide **2** at 1538 cm^{-1}; cycloepoxide and sulfonyl (O═S═O) asymmetric stretch at 1465 cm^{-1};[30] CF_2 and CF_3 stretching at 1389 cm^{-1}; C−O stretch and CF_2 stretching in the region of broad bands near 1000 cm^{-1}, bands attributed to C−F and possibly unreacted epoxide or alcohol at 980 cm^{-1}; and ostensibly another C−F signal at 926 cm^{-1}. Vibrational bands associated with sulfonyl fluoride S−F stretching bands are seen at 814 cm^{-1} and the C−F band at 724 cm^{-1}. Copolymer films containing sulfonyl fluoride epoxide **1** versus **3** show few distinct differences in these ATR-FTIR spectra.

Aqueous contact angle data is shown in Table 1 for copolymer films containing the commercial cycloaliphatic diepoxide **2** and fluorinated epoxide **3** in various compositions. The wetting data indicate relatively hydrophobic surfaces at all film compositions that are distinct from the film of pure cycloaliphatic diepoxide (41°, ref 28). Polar contributions from secondary hydroxyl and sulfonyl fluoride groups reduce the aqueous contact angles over what might otherwise be expected for a more hydrophobic fluorinated polymer.[24] The wetting data are consistent with an overlayer of the fluorinated epoxide exposed to air. Surface enrichment of perfluoro components is common where surface restructuring allows film components to rearrange to achieve equilibrium.[24−26] In this case, perfluorinated moieties have the lowest interfacial tension with air and move to occupy the interfaces in the cast monomer mixture prior to film polymerization. Hence, the data show that this hydrophobic fluorinated overlayer persists at the film surface to film bulk compositions very rich in the cycloaliphatic diepoxide.

Figure 3A shows a high-resolution XPS C_{1s} spectrum for a cast copolymer film comprising epoxide monomers **2** and **3** photopolymerized in roughly equal monomer ratios (48 wt % of **2**, 50 wt %, of **3** plus 2 wt % photoinitiator). XPS signals from residual propylene carbonate from the addition of photoinitiator UVI 6990 were deemed too small to distinguish from the other carbon signal contributions. The spectrum shows little hydrocarbon (285 eV signal) within the detection limit (tenths of atomic percent) for this sampling depth (50 Å). Even for polymerized samples such as this with "minimal" C−H XPS signal, the hydrocarbon peak was present and detectable, to permit adequate charge referencing to the hydrocarbon peak. Prominent, resolved peaks include those for ether carbon (287 eV), and various fluorinated species of carbon (C−F, 290 eV; CF_2, 293 eV; CF_3, 294 eV). Relatively strong perfluorinated carbon signals together with virtually nonexistent hydrocarbon signal for this sample strongly suggest high levels of enrichment of perfluorinated polymer segments in the outer atomic levels of the film. This important point is addressed further below.

Figure 3B displays the high resolution C_{1s} spectra for a homopolymer film of the commercial monomer **2** obtained by photoinitiation. The differences in XPS signatures between parts A and B of Figures 3 are clear: the homopolymer film of monomer **2** lacks the higher binding energy fluorocarbon peaks while the fluorinated polymer film lacks the carbonyl peak at 289 eV and the CH_x peak at 285 eV. Together, this comparison is useful for interpreting the XPS spectra for copolymer films of varying monomer composition shown in Figure 4.

(37) Brown, J. K.; Morgan, K. J. The Vibrational Spectra of Organic Fluorine Compounds. In *Adv. Fluorine Chem.*; Butterworth: London, 1965; Vol. 4, pp 253−314.

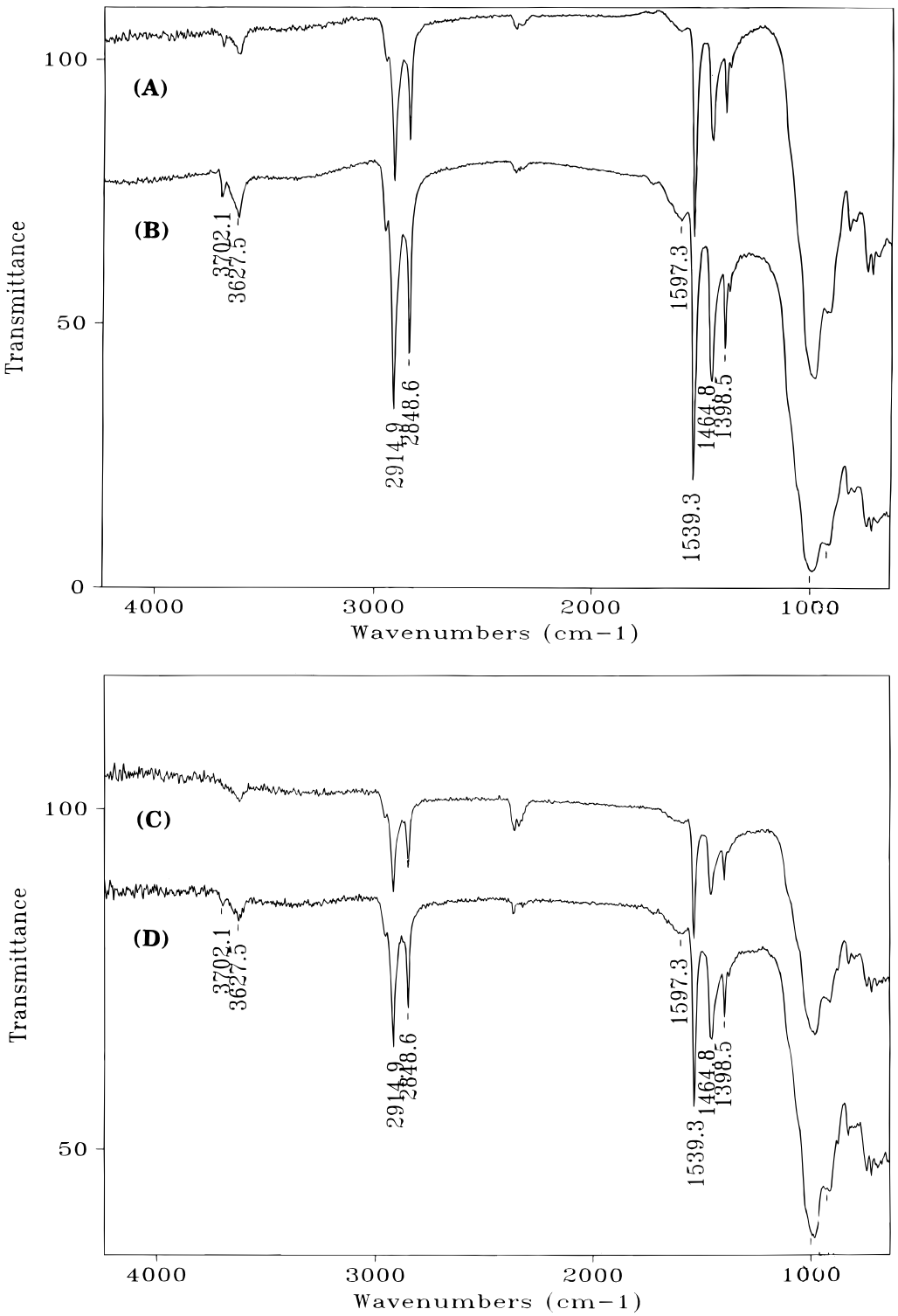

Figure 2. Attenuated total reflection FTIR spectra for photopolymerized epoxide films of various monomer mixtures and compositions: (A) 50 wt % fluorinated epoxide **3** and 48 wt % aliphatic diepoxide **2**; (B) 1 wt % fluorinated epoxide **3** and 97 wt % diepoxide **2**; (C) 50 wt % fluorinated epoxide **1** and 48 wt % diepoxide **2**; (D) 1 wt % fluorinated epoxide **1** and 97 wt % diepoxide **2**.

Compositional dependence of the XPS C_{1s} spectra for a series of epoxide copolymer containing monomers **2** and **3** in varying bulk compositions are shown in Figure 4. XPS spectra for films having high percentages of fluorinated epoxide **3** are shown at the top of the plot. Features characteristic of the sulfonyl fluoride monomer overlayer as described for Figure 3A are prominent for film compositions comprising 50, 30, and 17 wt % fluorinated epoxide monomer **3**. The chemical features associated with the cycloaliphatic epoxide **2** begin to appear in films having 17, 5, and 1 wt % monomer **3**. Nevertheless, peaks at 294 (CF_3), 293 eV (CF_2), and 290 eV (CF) remain strong, even down to 1 wt % of the fluorinated monomer, consistent with formation of a perfluorocarbon polymer overlayer when bulk monomer composition is dominated by nonfluorinated components.

Table 1 compiles the compositional data for polymerized films of varying monomer composition obtained by XPS analysis in Figure 3. A photopolymerized film of

Table 1. XPS Elemental Composition of Photopolymerized Epoxide Copolymer Films as a Function of Percent of $OCH_2CHCH_2OCF_2CF(CF_3)SO_2F$ (3) with Aliphatic Diepoxide (2)

sample	wt % monomer **3**	XPS atomic percent F	C	O	S	Cl[b]	contact angle (deg, H_2O, ±SD, $n = 10$)
A2	50	36.9	35.6	21.3	5.8	0.5	76 ± 4.4
B2	30	37.7	35.2	21.6	5.6		70 ± 3.2
C2	17	36.0	37.3	21.6	5.1		71 ± 2.0
D2	5	29.2	43.6	23.2	3.9		67 ± 2.1
E2	1	22.5	51.6	22.8	3.1		63 ± 1.5
theory[a]	100	38.9	33.3	22.2	5.6		
100% **2**	0	3.8	72.5	23.1	0.4		41 ± 2.1

[a] 100% monomer **3**. [b] Source of chlorine is residual allyl chloride used in preparation of monomers **1** and **3**.

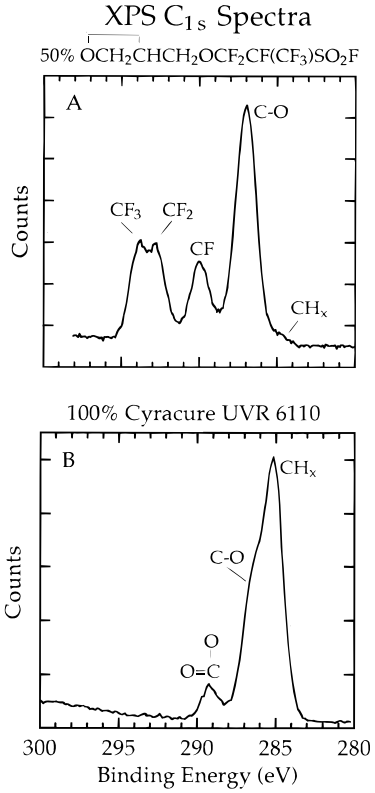

Figure 3. High-resolution XPS C_{1s} spectra for (A) a mixed photopolymerized film (A2) containing 50 wt % sulfonyl fluoride monomer **3** in 48 wt % **2**; (B) homopolymer film of **2**.

98 wt % aliphatic diepoxide monomer **2** with 2 wt % of UVI 6990 photoinitiator shows some evidence for the presence of the triaryl hexafluorophosphate sulfonium salt photoinitiator in the surface region (trace F and S XPS signals). When compared to the theoretical composition for a film of 100 wt % monomer **3**, copolymers of monomer **3** with monomer **2** show substantial nonstoichiometric increases in sulfur and fluorine content at their surface. This, in turn, reflects the enrichment of fluoroepoxide monomer **3** in the copolymer film outer surface. Since the depth sensitivity of the XPS signal is approximately 50 Å under these conditions, surface enrichment of the fluorinated epoxide **3** extends at least to this overlayer depth. A significant observation is that films polymerized with only 1 wt % monomer **3** (97 wt % monomer **2**) still display very high amounts of fluorine and sulfur on their surface. Also of interest is that for epoxide films containing equal amounts of monomer **2** and monomer **3**, a prepolymerization annealing step (55 °C under nitrogen) from 0.5 to 3 h, or changing UV intensity or irradiation times during curing does *not* change XPS-detected film surface composition (data not shown). This indicates that monomer migration, phase separation and surface enrichment occurs rapidly in cast monomer films prior to polymerization.

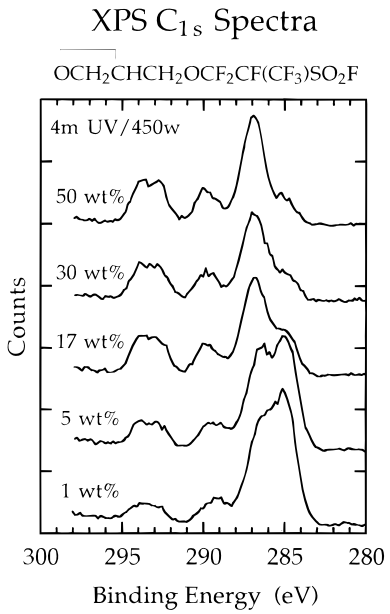

Figure 4. Compositional dependence of the XPS C_{1s} spectral region for a series of epoxide copolymer films containing fluorinated epoxide **2** and aliphatic epoxide **3** in various ratios.

Table 2. Depth-Dependent XPS Analysis for a Photopolymerized Film E2 Containing 1% $OCH_2CHCH_2OCF_2CF(CF_3)SO_2F$ (3), 2% UVI 6990 Photoinitiator, and 97% Cyracure Diepoxide (2)

takeoff angle	sampling depth (Å)	XPS atomic percent F	C	O	S
80	15	28.4	46.0	21.9	3.8
55	50	18.2	56.9	22.8	2.1
0	90	13.0	60.6	23.1	1.4
theory[a]		38.9	33.3	22.2	5.6

[a] 100% SO_2F monomer **3** film.

Table 2 shows results for angular-resolved XPS experiments on a copolymer film containing 1 wt % fluorinated epoxide monomer **3** and 97 wt % cycloaliphatic diepoxide **2** (plus 2 wt % photoinitiator). Three different angles were used, resulting in composition information from 15, 50, and 90 Å sampling depths. These data show that both fluorine and sulfur species have their highest concentrations at the film's surface. Again, this strongly supports a gradient of increasing fluorocarbon content from the bulk to the film surface. A depth profile plotting the compositional trends in this film as a function of depth is plotted in Figure 5. This profile is calculated from the XPS angle-resolved data using an improved regularization algorithm.[38,39] As predicted by Table 2, Figure 5 explicitly shows the calculated gradient of fluorocarbon content increasing toward the surface. The S, F, C, and O concentrations are close to the values expected for 100% monomer **3** at the outermost surface layer. The sulfur and fluorine

(38) Tyler, B. J.; Begaye, E. M. in preparation.
(39) Tyler, B. J.; Castner, D. G.; Ratner, B. D. *Surf. Interface Anal.* **1989**, *14*, 443.

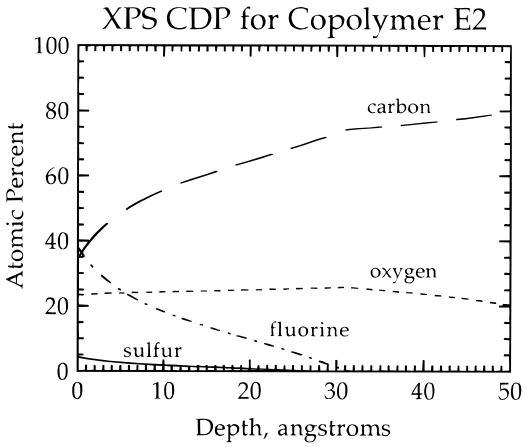

Figure 5. Compositional depth profile constructed from XPS data for an epoxide copolymer prepared from 97 wt % monomer **2** and 1 wt % monomer **3**.

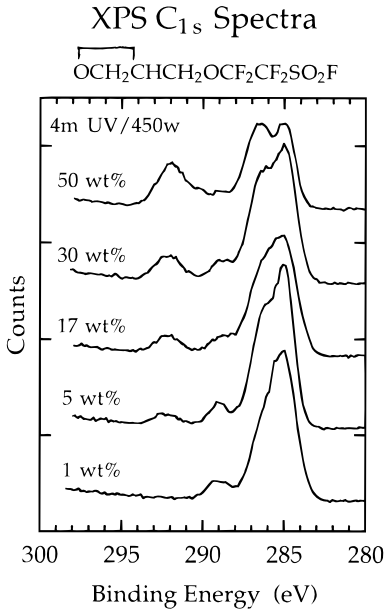

Figure 6. Compositional dependence of the XPS C_{ls} spectral region for a series of epoxide copolymer films containing fluorinated epoxide **1** and aliphatic epoxide **2** in various ratios.

concentrations drop to zero within 30 Å of surface, leaving the C and O concentrations at values close to those of the pure diepoxide **2**. These data document the high surface enrichment of fluoroepoxide **3**, even at a 1 wt % level in bulk.

A similar set of data has been collected for copolymerized films of fluorinated epoxide **1** and diepoxide **2**. Figure 6 displays the compositional dependence of the XPS C_{1s} region for films comprising fluorinated monomer **1** and diepoxide **2** for a series of bulk compositions. In comparison to fluorinated monomer **3** and Figure 4, the compositional dependence of the XPS data for monomer **1** is not as distinct. Films of monomers **1** and **2** in equal proportions still show strong evidence of high fluorinated epoxide enrichment in the outer surface. Yet, as the amount of fluorinated monomer decreases, the characteristic signals for the hydrocarbon diepoxide monomer **2** (e.g., CH_x peak at 285 eV) grow into the spectra significantly, becoming more dominant at richer fluoromonomer film contents than seen in Figure 4. At 1 wt % fluorinated monomer **1** content, fluorinated carbon species were not detected in the C_{1s} spectrum—a

Table 3. XPS Elemental Composition of Photopolymerized Epoxide Copolymer Films as a Function of Percent of $OCH_2CHCH_2OCF_2CF_2SO_2F$ (1)

sample	wt % monomer **1**	XPS atomic percent F	C	O	S	Cl[b]	contact angle (deg, H_2O, ±SD, $n = 10$)
F2	1	2.4	75.3	21.8		0.5	61 ± 1.1
G2	5	12.1	62.5	22.4	2.0	1.1	62 ± 4.5
H2	17	17.1	55.5	23.6	2.9	1.0	61 ± 4.8
I2	30	19.6	52.8	23.8	2.8	1.0	65 ± 3.6
K2	50	27.9	44.8	19.5	3.7	4.2	62 ± 4.7
theory[a]	100	33.3	33.3	26.7	6.7		
100% **2**	0	3.8	72.5	23.1	0.4		41 ± 2.1

[a] 100% epoxide SO_2F monomer **1** film. [b] Source of chlorine is residual allyl chloride used in preparation of monomers **1** and **3**.

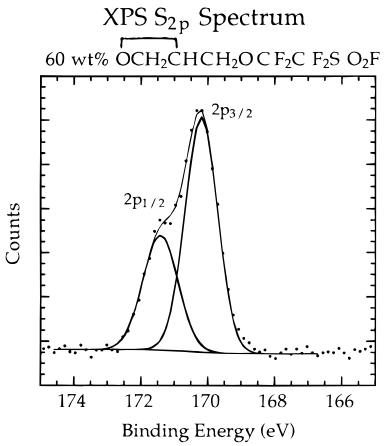

Figure 7. XPS S_{2p} spectrum for a photopolymerized epoxide copolymer film containing 60% sulfonyl fluoride monomer **1**.

stark contrast to the case for monomer **3** where perfluorocarbon peaks were observed at all film compositions. This suggests that the fluorinated monomer surface enrichment is not as favored in this case, resulting in less surface overlayer formation. These data are summarized in Table 3 with specific elemental composition breakdown for all elements detected. All films exhibit detectable, significant fluorine surface enrichment, with films of equal proportions of monomers **1** and **2** showing surfaces similar chemically to a film of 100 wt % fluorinated epoxide. Surface enrichment in this film remained unaffected by precure annealing at 55 °C or changing irradiation times or intensity. For a mixed ternary epoxide copolymer film comprising 2 wt % sulfonyl fluoride monomer **3** and 3 wt % sulfonyl fluoride monomer **1** and the balance of the mixture being aliphatic cyclodiepoxide **2**, the XPS elemental composition is 28.8% F, 44.4% C, 23.2% O, 3.3% S, and 0.3% Cl (chlorine signal attributed to residual allyl chloride used in the preparation of monomers **1** and **3**). This is very close to the surface composition for 5 wt % of monomer **3** shown in Table 1. This supports all other data for film surface enrichment.

Contact angle data shown in Table 3 are consistent with XPS for these systems, showing increased aqueous wettability versus films containing sulfonyl fluoride monomer **3**, in agreement with reduced fluorine enrichment seen in these films by XPS. Nevertheless, wettability is decreased over that seen for pure cycloaliphatic epoxide films,[28] supporting the limited presence of the fluorinated epoxide in the surface region.

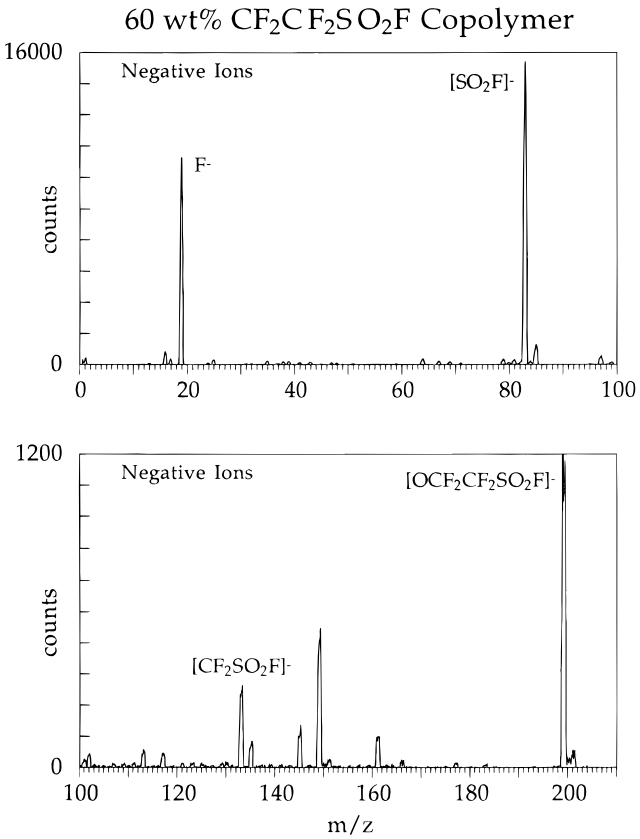

Figure 8. Negative static SIMS spectrum for a photopolymerized copolymer film prepared from 60 wt % monomer **1** and 38 wt % monomer **2**.

The high-resolution S_{2p} binding region for a polymer film containing 60 wt % fluorinated monomer **1** is shown in Figure 7. Sulfur $2p_{3/2}$ binding energy for the sulfonyl group is 170.3 eV, shifted 2 eV higher in binding energy than typical sulfonyl compounds. This 2 eV shift is likely due to the strong electron-withdrawing power of the F substituent attached to sulfur. This lends additional support for the presence of the $-SO_2F$ group at the surface of these films.

Static SIMS experiments were done on copolymer films made from monomers **1** and **2**. Although both positive and negative secondary ion spectra were obtained, the negative ions were the most informative. A representative negative static SIMS spectrum is shown in Figure 8. The most intense peaks in the negative secondary ion spectra were observed at m/z = 19, 83, and 199. These values are consistent with $[F]^-$, $[SO_2F]^-$, and $[OCF_2CF_2SO_2F]^-$ fragments from monomer **1**, indicating its presence at the surface of the copolymer films since the sampling depth of static SIMS is ca. 15 Å. Other smaller peaks in the spectrum can also be assigned to fragments of monomer **1**. For example, the peak at m/z = 133 is consistent with the fragment $[CF_2SO_2F]^-$. A small peak at m/z = 80, characteristic of $[SO_3]^-$, is barely visible above the noise, reflecting the lack of conversion of $-SO_2F$ to other oxidized surface species under these conditions. The positive ion static SIMS spectra comprised primarily hydrocarbon and fluorocarbon fragments.

Conclusions

The array of surface analysis methods directed at photoinitiated copolymerized films cast from mixtures of fluorinated sulfonyl fluoride epoxide monomers and a commercial aliphatic diepoxide indicate that the fluorinated monomer migrates to the film−air interface. This leads to nonstoichiometric enrichment of the film surface with fluorinated monomer bearing sulfonyl fluoride groups. The surface segregation effect is more prominent for fluorinated epoxide monomer **3**, bearing an extra pendant $-CF_3$ group not found in fluorinated epoxide **1**. Surface enrichment of fluorinated monomer **3** leads to formation of a prominent fluorinated polymer overlayer in all film compositions down to 1 wt % fluorinated monomer (97 wt % aliphatic bulk monomer content). This overlayer forms only at highly-to-moderately rich compositions of fluoromonomer **1** in mixed copolymer films.

The potential to fabricate highly enriched fluoropolymer films bearing surface exposed sulfonyl fluoride groups has been demonstrated. Such a strategy allows a route to forming fluoropolymer overlayer coatings using only minor amounts of relatively expensive or exotic fluorinated monomer in conventional commercial aliphatic polymer resins.

Acknowledgment. K. Hinds and J. Caballero provided assistance with FTIR and contact angle measurements. Support is gratefully acknowledged from National Science Foundation/EPRI joint grant program (NSF MSS-9212496 and EPRI RP-8017) (D.W.G.), National Science Foundation Grant DMR-9357439 (D.W.G.), Tektronix, Inc. (D.W.G.), and National Institutes of Health Grant RR-01296 (D.G.C.).

CM960049X